

The impact of iron oxide magnetic nanoparticles on the soil bacterial community

Shiying He · Youzhi Feng · Hongxuan Ren · Yu Zhang ·
Ning Gu · Xiangui Lin

Received: 2 May 2011 / Accepted: 4 August 2011
© Springer-Verlag 2011

Abstract

Purpose Iron oxide magnetic nanoparticles (IOMNPs) have numerous exciting applications due to their unique chemical and physical properties. With increased applications of engineered nanostructures, releases of such materials to soil are undoubtedly inevitable. Their potential environmental risks have attracted increasing concern. One area of concern is their effect on microorganisms, which are important components of ecosystems.

Materials and methods In this work, the effect of IOMNPs (Fe_3O_4 and $\gamma\text{-Fe}_2\text{O}_3$) on the soil bacterial community has been studied with molecular approaches and enzyme analyses. The community structure and population size were analysed using molecular-based methods, including PCR-denaturing gradient gel electrophoresis and real-time quantitative PCR based on the universal bacterial biomarker,

the 16S rRNA gene sequence fragment for the bacterial variable V3 region. In addition, plate counting was conducted to validate the results of molecular methods. Four enzyme activities (dehydrogenase, urease, invertase and phosphatase) involved in cycling the main biologically important nutrients (C, N and P) were measured.

Results and discussion Our analysis revealed that the addition of IOMNPs could potentially stimulate some bacterial growth and change the soil bacterial community structure, although bacterial abundance does not change. Based on molecular fingerprinting and sequencing analysis, several potential IOMNPs-stimulated bacteria were related to Actinobacteria, such as Duganella, Streptomyetaceae or Nocardioideae. Meanwhile, soil urease and invertase activities significantly increased under IOMNPs amendment, which could be a consequence of the changes in the bacterial community.

Conclusions Molecular evidence suggests that IOMNP addition may facilitate C and N cycling in soil by influencing soil bacterial community. These findings are of great help towards building a comprehensive understanding of the potential impact of nanoparticles on the environment.

Responsible editor: John W. G. Cairney

The first two authors have the equivalent contributions to the manuscript.

Electronic supplementary material The online version of this article (doi:10.1007/s11368-011-0415-7) contains supplementary material, which is available to authorized users.

S. He · Y. Zhang · N. Gu (✉)
Jiangsu Laboratory for Biomaterials and Devices,
School of Biological Science and Medical Engineering,
Southeast University, Nanjing 210096, People's Republic of China
e-mail: guning@seu.edu.cn

Y. Feng · X. Lin
State Key Laboratory of Soil and Sustainable Agriculture,
Institute of Soil Science, Chinese Academy of Sciences,
Nanjing 210008, Jiangsu Province, People's Republic of China

H. Ren
National Center for Nanoscience and Technology of China,
Beijing 100080, People's Republic of China

Keywords DGGE · Iron oxide magnetic nanoparticles · Soil bacterial community

1 Introduction

Iron oxide magnetic nanoparticles (IOMNPs) are one of the most widely studied and applied nanomaterials. Due to their novel properties, such as enhanced surface-to-volume ratio, superparamagnetism and inherent biocompatibility (Sjogren et al. 1997; Perez et al. 2002), IOMNPs have a

wide variety of applications, including use in medical diagnostics, controlled drug release, separation technologies and environmental engineering. As manufacturers increase their nanomaterial production to meet ever-increasing demands, the release of such materials into soil is inevitable (Nowack 2009; Ju-Nam and Lead 2008; Lee et al. 2010). Increasing concerns have been raised on how this release would affect ecosystem health and human safety (Meng et al. 2009; Klaine et al. 2008; Colvin 2003). Unfortunately, little knowledge is available to date despite these concerns. A paramount aspect of understanding this impact is to determine how microorganisms respond to IOMNPs because these organisms are an indispensable part of the environment.

Microorganisms are the drivers of global biogeochemical cycles. They are involved in the cycling of carbon, nitrogen, sulphur and phosphorus. Because microorganisms are especially sensitive to environmental changes (Sadowsky and Schortemeyer 1997), the structure and abundance of the microorganism community may shift in response to foreign nanomaterials (Ge et al. 2011; Kumar et al. 2011; Tong et al. 2007). Because microorganisms help regulate and maintain overall ecosystem health and function (Kaye et al. 2005; Janvier et al. 2007), changes in the microbial community will have a great effect on the entire ecosystem (Kanerva et al. 2008). Therefore, a better understanding of how microorganisms respond to nanomaterials can help to address environmental and health concerns brought about by the manufacture and use of nanomaterials.

Many nanomaterials, such as carbon nanotubes (Kang et al. 2007; Liu et al. 2009), graphene-based nanomaterials (Hu et al. 2010), iron-based nanoparticles (Auffan et al. 2008), silver (Sondi and Salopek-Sondi 2004) and copper, zinc and titanium oxide nanoparticles (Kasemets et al. 2009), have been reported toxic effects on pure cultures of bacteria. Due to the existence of multiple factors in complicated environments such as soil, investigations of the effects of nanoparticles on bacteria *in situ* are more meaningful than those under pure culture. However, there are limited and inconsistent data regarding the effect of nanoparticles on the soil microbial community. For instance, fullerenes have little impact on the structure and function of the soil microbial community (Tong et al. 2007), whereas nano-TiO₂ and ZnO have negative effects on soil bacterial communities (Ge et al. 2011). In this study, we investigated the effect of IOMNPs (Fe₃O₄ and γ -Fe₂O₃) on the bacterial community in soil microcosms. The community structure and population size were analysed using molecular-based methods, including PCR-denaturing gradient gel electrophoresis (PCR-DGGE) and real-time quantitative PCR (qPCR) based on the universal bacterial biomarker, the 16S rRNA gene sequence fragment for the bacterial variable V3 region. In addition, plate counting was

conducted to validate the results of molecular methods. The effects of IOMNPs on nutrient cycling were also evaluated. Four enzyme activities (dehydrogenase, urease, invertase and phosphatase) involved in cycling the main biologically important nutrients (C, N and P) were measured. Our findings offer a relatively comprehensive assessment of the impact of IOMNPs on the soil environment.

2 Experimental section

2.1 Preparation of IOMNPs

Fe₃O₄ nanoparticles were synthesised by the chemical coprecipitation method. Typically, a solution of FeCl₃ and FeSO₄ (molar ratio 2:1) was prepared under N₂, followed by the slow addition of a sufficient amount of aqueous ammonia solution with vigorous stirring for 30 min. The black Fe₃O₄ precipitates were obtained and washed immediately with distilled water five times using magnetic separation. The final precipitates were dispersed in distilled water at a concentration of 0.128 M and pH 3.0 and oxidised into more stable γ -Fe₂O₃ by air at 90°C. Nanoparticles were washed for five times with distilled water by magnetic separation to remove residual iron ions. Then, IOMNPs were resuspended in distilled water (obtaining about 2 mg ml⁻¹), sterilized through a 0.22- μ m sterilized filter and stored at 4°C for use.

The particle size and morphology were determined by transmission electronic microscopy (TEM, JEOL, JEM-2000EX) operated at an accelerating voltage of 120 kV. Five microliters of the nanoparticles suspension was placed on the carbon-coated copper grids, and the solvent was allowed to evaporate. The nanoparticles diameter distribution was determined with image software by analysing greater than 400 particles. IOMNPs were sonicated for 20 min so that the particles could be uniformly dispersed. All other chemicals were of reagent grade and used as received without further purification. Double distilled water was used for all experiments.

2.2 Sample collection, treatment and toxicity assay

The soil samples used for evaluating the effects of IOMNPs on the diversity of bacterial community structure were collected from a vegetable field located in Yixing County, Jiangsu Province in China's Yangtze River Delta. The soil is classified as an Anthrosol. Fresh soil samples were stored at 4°C. The soil was mixed and sieved through a 2-mm mill. Each microcosm contained 50 g dry weight soil (d.w.s) in a 250-ml vial. The vials were closed with filters, thereby allowing maintenance of stable humidity conditions and permitting ventilation. Next, the Fe₃O₄ and γ -Fe₂O₃ nano-

particles were added to the soil. For both Fe_3O_4 and $\gamma\text{-Fe}_2\text{O}_3$ nanoparticles, 0.42, 0.84 and 1.26 mg g^{-1} d.w.s were studied, which were commonly used in the study of nanomaterials behaviour in environment (Ge et al. 2011). To ensure that nanoparticles were thoroughly mixed into the soil, the distilled water containing the appropriate amount of IOMNPs was added drop wise to soil surface, following the protocol of Jia and Conrad (2009). Microcosms without IOMNPs were used as controls. The experiments were conducted at 60% maximum water-holding capacity, 25°C and in darkness. Humidity was maintained by adding sterile distilled water to replace the water lost to evaporation during aeration. Destructive sampling was carried out at time zero and after 15 and 30 days of incubation, respectively, and three replicates for each sample were taken.

2.3 DNA extraction, PCR-DGGE analysis of bacterial 16S rRNA gene sequences

For each sample and each triplicate, 0.5 g soil was used to extract genomic DNA on the day after sampling by using the FastDNA® SPIN Kit (MP Biomedicals, Santa Ana, CA) according to the manufacturer's instruction. The extracted soil DNA was dissolved in 50 μl TE buffer, quantified by spectrophotometer and stored at -20°C until further use. An ~ 200 -bp fragment of the V3 region of the small subunit of the 16S rRNA gene was amplified using the primer set for bacteria as previously described in detail (Muyzer et al. 1993). Briefly, the forward primer was 341F (5'-CCTACGGGAGG-CAGCAG-3'), and the reverse primer was 534R (5'-ATTACCGCGGCTGCTGG-3'). A 40-nucleotide GC-rich sequence (GC-clamp) was added to the forward primer (5'-CGCCCCCGCGCGCGCGGGCGGGGCGGGGGCAC-GGGGGG-3'). The programme parameters were as follows: initial denaturation, 94°C for 5 min; (denaturation, 94°C for 30 s; annealing, 55°C for 30 s; elongation, 72°C, 30 s) \times 30 cycles; followed by a final elongation of 72°C for 10 min.

A DCode Universal Mutation Detection System (Bio-Rad, Hercules, CA) was used for DGGE analysis. Approximately ca. 200 ng of bacterial PCR amplicons of 16S rRNA gene fragments from each sample were electrophoresed on an 8% (w/v) acrylamide–bisacrylamide gel with 30% to 70% denaturant (where the 100% denaturant contains 7 M urea and 40% (vol/vol) formamide) at 130 V for 8 h in 1 \times TAE running buffer at 60°C. Next, the gel was stained for 30 min with SYBR Green I nucleic acid gel stain (Cambrex Bio Science, Rockland, ME.) and then visualised using a Gel Doc™ EQ imager combined with Quantity one 4.4.0 (Bio-Rad). Band intensities were digitalised. Dominant DGGE bands were excised and eluted overnight in sterilised Milli-Q water at 4°C, re-amplified and run again on the DGGE system to ensure the

purity and correct mobility of the excised DGGE bands. PCR products were purified using the QIAquick PCR purification kit (QIAGEN) before cloning.

2.4 Cloning, sequencing and phylogenetic analysis

The purified DNA amplicons of the excised DGGE bands were cloned into a pMD18-T vector (TaKaRa, Japan) and transformed into *Escherichia coli* DH5 α competent cells. Three random clones containing the correct size gene for each DGGE band were sequenced by the Invitrogen Sequencing Company in Shanghai. DNASTAR software package was used to manually check and compare the clone sequences. One representative clone sequence over 98% DNA identity after sequence comparison from each band was used for the phylogenetic analysis.

The top three BLAST hits and the bacterial 16S rRNA gene sequences were used to build a basic phylogenetic tree by the neighbour-joining method using MEGA 4.0 (Molecular Evolutionary Genetics Analysis) (Tamura et al. 2007). The tree topology was further evaluated by different methods including minimum evolution and maximum parsimony. The phylogenetic relationship of the bacterial 16S rRNA gene sequences to the closest homolog in GenBank was then inferred.

2.5 Nucleotide sequence accession numbers

Sequences generated during this study have been deposited in the DDBJ database under accession numbers AB525872–AB525883.

2.6 Real-time quantitative PCR of bacterial 16S rRNA genes in soils

Real-time qPCR was used to determine the population size of bacteria. The detailed protocol was described previously by Feng et al. (2009). Briefly, the copy number of soil bacterial 16S rRNA genes was quantified by qPCR analysis with an Opticon 2 continuous fluorescence detection system (MJ Research). To generate a standard curve, a single clone containing the correct insert of bacterial 16S rRNA gene was grown in LB medium, and then plasmid DNA was extracted, purified and quantified. A 10-fold dilution series of the plasmid DNA was made to generate a standard curve of bacterial 16S rRNA gene covering six orders of magnitude from 1.0×10^3 to 1.0×10^8 copies of the template per assay. Assays were set up using the SYBR *Premix Ex Taq*™ Kit (TaKaRa). The 25- μl reaction mixture contained 12.5 μl of SYBR® *Premix Ex Taq*™, 0.5 μM of each primer, 200 ng BSA μl^{-1} and 1.0 μl template containing approximately 2–9 ng DNA. Blanks were always run with water as the template in place of a soil

DNA extract. Specific amplification of bacterial 16S rRNA gene was confirmed by agarose gel electrophoresis of real time PCR amplicons showing the expected band size and having a melting curve that always resulted in a single peak. Real-time PCR was performed in triplicate, and amplification efficiencies of 97.4–104% were obtained with R^2 values of 0.966–0.977. Based on the standard curve plotted using the known bacterial 16S rRNA gene copy number against the cycle threshold (C_T), the copy number of bacterial 16S rRNA gene in the soil DNA extract was calculated by extrapolating the C_T value at which its fluorescence emission crossed a threshold within the logarithmic increase of bacterial 16S rRNA gene in the soil. The threshold was defined as 10 times the standard deviation around the average intensity of background fluorescence. The final bacterial 16S rRNA gene quantities were obtained by calibrating against the total DNA concentration extracted and the soil water content.

2.7 Enzymatic activities

Soil enzyme activities were determined in triplicate. Subsamples were collected after 0, 5, 10, 15, 20 and 30 days incubation. Invertase activity was determined with sucrose as a substrate; reducing sugars were analysed as described by Schinner and Vönmersi (1990). Phosphatase activity was evaluated described by Dick et al. (2000). The activities of soil urease and dehydrogenase were determined as described by Tabatabai (1994).

2.8 Statistical analysis

Statistical procedures were carried out with the software package SPSS 13.0 for Windows. Data are expressed as means with standard deviation (SD), and the letters above error bars indicate statistical differences between the values of different treatments. Mean separation was conducted based on Tukey's multiple range test after the global one-way ANOVA. Differences at $p < 0.05$ were considered statistically significant.

DNA fingerprints obtained from the bacterial 16S rRNA gene banding patterns on the DGGE gels were photographed and digitised using Bio-Rad's Quantity One software. Principal component analysis was carried out, and all of the DGGE bands were used in the calculation. Principal component analysis was performed using EXCEL STATISTICS 97.

3 Results

3.1 TEM analysis of IOMNPs

The typical TEM images of IOMNPs (Fig. 1) show aggregations due to drying on the TEM grid or aggregation

in the suspension. However, individual particles of quasi-spherical shape were observed. The size distribution of nanoparticles was measured. The mean diameter of particles was found to be approximately 10.5 nm (Fe_3O_4) and 10.2 nm ($\gamma\text{-Fe}_2\text{O}_3$). Use of particles of the same morphology and size distribution ensure that eventually effect differences between the two types of nanoparticles are due to their chemical characteristics.

3.2 DGGE fingerprinting profiles and phylogenetic identification of bacterial 16S rRNA gene

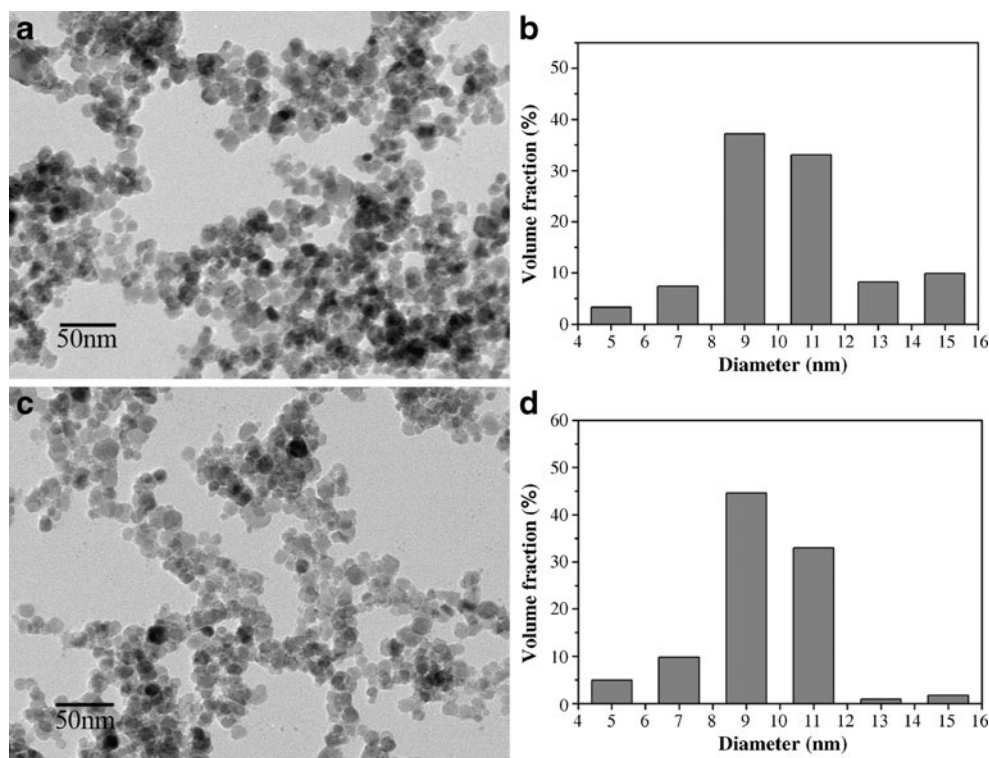
DNA fingerprinting pattern differences have been demonstrated to be useful in assessing the consequences of introduced chemicals on soil microbial community structure (Kirk et al. 2004; O'Donnell et al. 2001). In Fig. 2, several dominant bands of 16S rRNA genes appeared consistently in soil samples from all treatments (i.e., bands 2, 3, 4, 5, 9 and 12), regardless of treatment with IOMNPs. The phylogenetic tree (Fig. 3) illustrates that these representative bands are related to Oxalobacteraceae, Intrasporangium, Terrabacter and/or Bacillus. Meanwhile, some DGGE bands appeared under IOMNPs amendments. The bands induced by IOMNPs treatment are 1, 6, 7, 8, 10 and 11, which are related to Duganella, Streptomyetaceae and/or Nocardioides. These results may indicate that IOMNPs addition changes soil bacterial community structure via promoting growth of some bacteria in soil. With visual comparison, the soil bacterial community structure seems similar at 15 and 30 days, suggesting that the shifts in bacterial community structure induced by IOMNPs treatment occurred within 15 days.

Of the two nanoparticles, $\gamma\text{-Fe}_2\text{O}_3$ seems to exert greater influence on the bacterial community structure. For example, six DGGE bands (1, 6, 7, 8, 10 and 11, mainly grouped into Streptomyces) appeared under $\gamma\text{-Fe}_2\text{O}_3$ treatments, whereas only two bands (8 and 11) appeared under Fe_3O_4 treatment. In addition, DGGE profiles reveal concentration-dependent effects of $\gamma\text{-Fe}_2\text{O}_3$ on bacterial community structure. The digital band intensities of bands 1, 7, 8, 9, 10, 11 and 12 seem to increase by at least 19% with 0.84 mg g^{-1} d.w.s of $\gamma\text{-Fe}_2\text{O}_3$, compared with those treated with 0.42 or 1.26 mg g^{-1} d.w.s. The unique DGGE band 6 had the highest band intensity at the 1.26 mg g^{-1} d.w.s level of $\gamma\text{-Fe}_2\text{O}_3$. In contrast, the intensities of several DGGE bands (2, 3, 4 and 5) decreased by at least 32% when treated with 1.26 mg g^{-1} d.w.s of $\gamma\text{-Fe}_2\text{O}_3$.

3.3 Principal component analysis of treatment of the bacterial community with IOMNPs

Principal component analysis (PCA) (Fig. 4) of the effects of IOMNP treatment on DGGE patterns clearly showed

Fig. 1 TEM images of IOMNPs. **a** Fe₃O₄, **c** γ-Fe₂O₃ and their relative size distribution (**b, d**). The mean diameter of the IOMNPs was 10.5 nm (Fe₃O₄) and 10.2 nm (γ-Fe₂O₃). The intensity scale on the y-axis represents the volume fraction of each size



differences in the bacterial community between IOMNP-treated and untreated samples. Additionally, there was a greater effect of γ-Fe₂O₃ than Fe₃O₄ on the bacterial community structure. The first principal component differentiated bacterial communities in γ-Fe₂O₃-treated soils from controls, which suggests that γ-Fe₂O₃ made the largest contribution to differences in the bacterial community composition between treated soils and control samples (46.4% of contribution rate). The bacterial community structure with Fe₃O₄ treatment was similar to that of

controls, which indicated a slight change in bacterial communities between Fe₃O₄-treated soils and controls. The distances between different IOMNPs concentrations and controls were varied along the second principal component axis; the greatest change in bacterial community was observed at 0.84 mg g⁻¹ d.w.s γ-Fe₂O₃. Meanwhile, 1.26 mg g⁻¹ d.w.s γ-Fe₂O₃ had a greater effect than 0.42 mg g⁻¹ d.w.s γ-Fe₂O₃. Among the Fe₃O₄ treatments, 1.26 mg g⁻¹ d.w.s Fe₃O₄ nanoparticles had the greatest effect on the structure of the soil bacterial community.

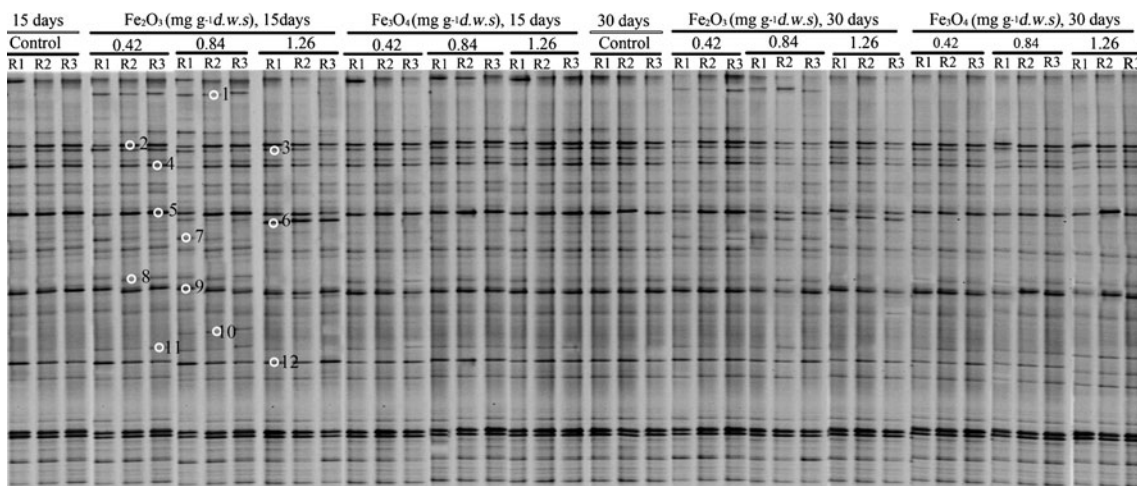
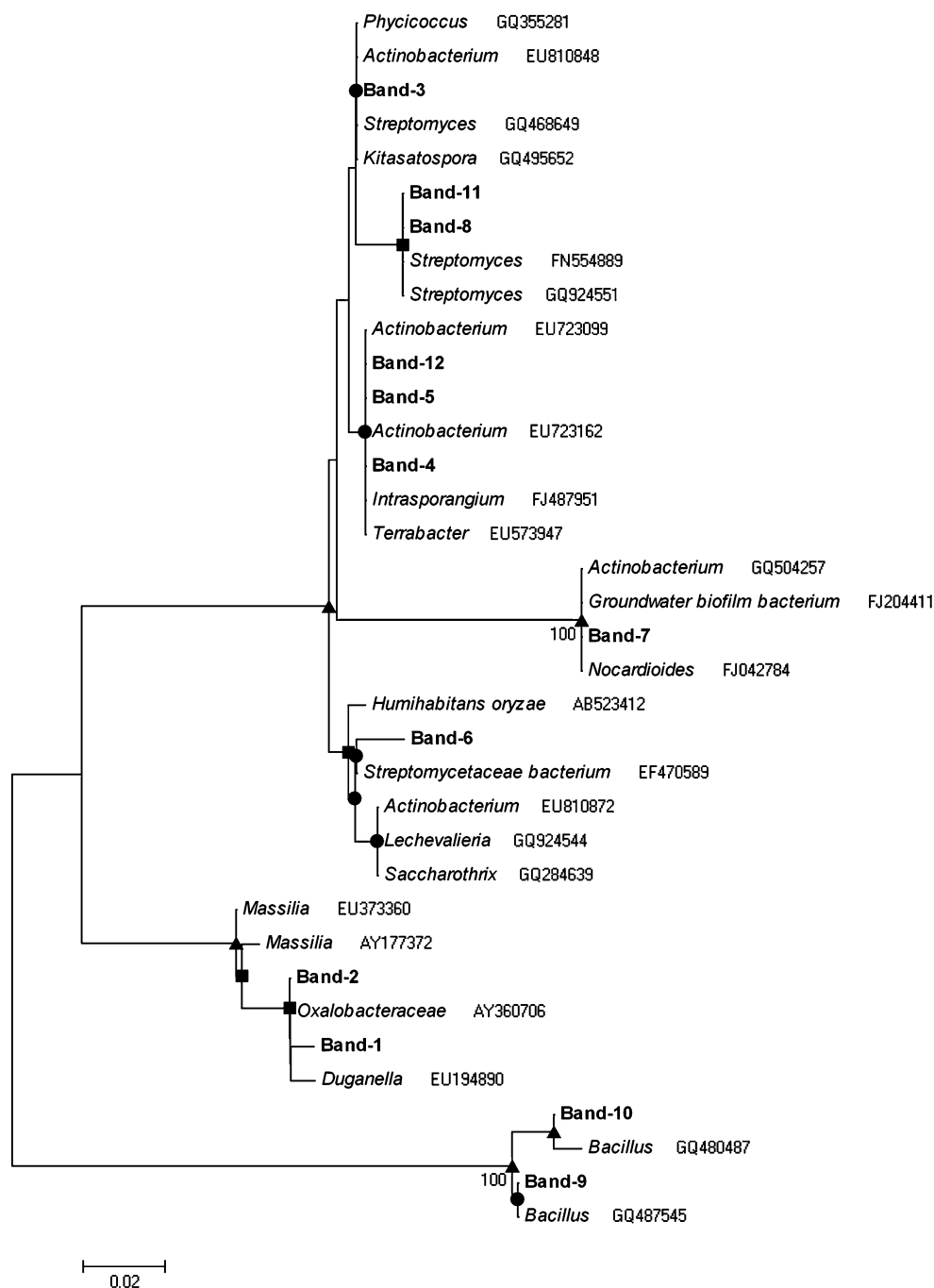


Fig. 2 DGGE fingerprinting profiles of 16S rRNA gene in soils treated with different concentrations of IOMNPs (Fe₃O₄ and γ-Fe₂O₃). Sample designations are indicated above each DGGE lane. The bands excised for sequencing are circled and numbered from 1 to 12

Fig. 3 Phylogenetic tree analysis showing the relationships of 200-bp 16S rRNA genes fragments in soil with the closest relatives deposited in GenBank. Bootstrap values are indicated as *black circles* (50–70%), *black square* (71–90%) and *black triangle* (>90%). Scale bar indicates the number of nucleotide acid substitutions per site



3.4 Quantitative analysis of soil bacterial abundance by qPCR and plate counting

The effects of IOMNPs on the population size of the bacterial community were measured by qPCR (Fig. 5) and plate counting (Electronic Supplementary Material). The qPCR results indicated that the abundance of the soil bacterial community did not change significantly in the microcosms containing soil and IOMNPs. The amount of bacteria culturable on nutrient agar also showed a similar pattern. For the incubation time-course, the same pattern

was detected between 15 and 30 days. However, the effects of γ -Fe₂O₃ and Fe₃O₄ on the population size of bacteria were different. The number of soil bacteria in the samples treated with γ -Fe₂O₃ appeared to be slightly larger than that of the samples treated with Fe₃O₄.

3.5 Enzyme activity

The results of the enzyme assays for soils incubated with or without IOMNPs are shown in Fig. 6. There were potentially positive responses in soil enzyme activities to

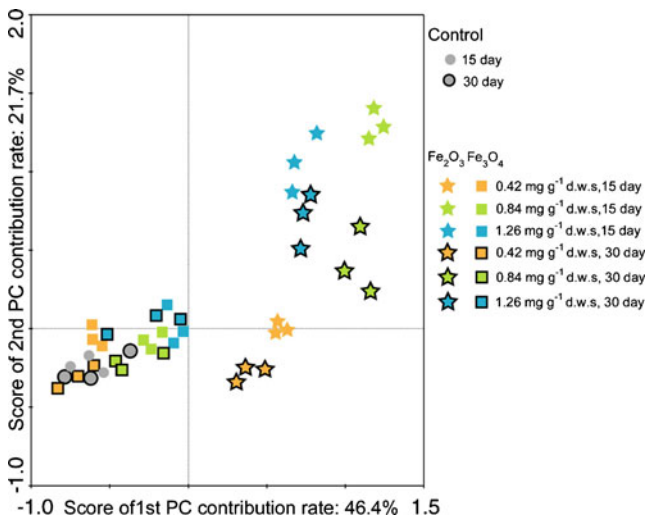


Fig. 4 Principal component analysis of the 16S rRNA gene banding profiles for bacteria from the soil amended with different concentrations of IOMNPs (Fe_3O_4 and $\gamma\text{-Fe}_2\text{O}_3$). The contribution rates of the first and second principal component (PC) are 46.4% and 21.7%, respectively

IOMNPs treatment. Invertase and urease activities in $\gamma\text{-Fe}_2\text{O}_3$ treatments ($28.6\text{--}29.1\text{ mg g}^{-1}\text{ glucose d.w.s day}^{-1}$ and $0.357\text{--}0.372\text{ mg NH}_3\text{-N g}^{-1}\text{ d.w.s day}^{-1}$) were significantly higher than those in controls ($24.9\text{--}25.6\text{ mg g}^{-1}\text{ glucose d.w.s day}^{-1}$ and $0.314\text{--}0.328\text{ mg g}^{-1}\text{ NH}_3\text{-N d.w.s day}^{-1}$); they were significantly highest at the 0.84 and $1.26\text{ mg g}^{-1}\text{ d.w.s}$ concentrations ($p < 0.05$). Furthermore, the values of the activities of invertase and urease were also significantly higher with $\gamma\text{-Fe}_2\text{O}_3$ treatment than those with Fe_3O_4 treatment ($23.4\text{--}26.1\text{ mg g}^{-1}\text{ glucose d.w.s day}^{-1}$ and $0.311\text{--}0.349\text{ mg g}^{-1}\text{ NH}_3\text{-N d.w.s day}^{-1}$), indicating that $\gamma\text{-Fe}_2\text{O}_3$ addition had a greater impact on enzyme activities.

Dehydrogenase and phosphatase activities in $\gamma\text{-Fe}_2\text{O}_3$ treatments ($111.3\text{--}113.2\text{ }\mu\text{g g}^{-1}\text{ TPF d.w.s day}^{-1}$ and $1.98\text{--}2.04\text{ mg g}^{-1}\text{ hydroxybenzene d.w.s day}^{-1}$) and in Fe_3O_4 treatments ($104.7\text{--}106.9\text{ }\mu\text{g g}^{-1}\text{ TPF d.w.s day}^{-1}$ and $1.93\text{--}1.96\text{ mg g}^{-1}\text{ hydroxybenzene d.w.s day}^{-1}$) were both not influenced by IOMNPs and were similar to those in controls ($104.3\text{--}105.3\text{ }\mu\text{g g}^{-1}\text{ TPF d.w.s day}^{-1}$ and $1.88\text{--}1.93\text{ mg g}^{-1}\text{ hydroxybenzene d.w.s day}^{-1}$).

4 Discussion

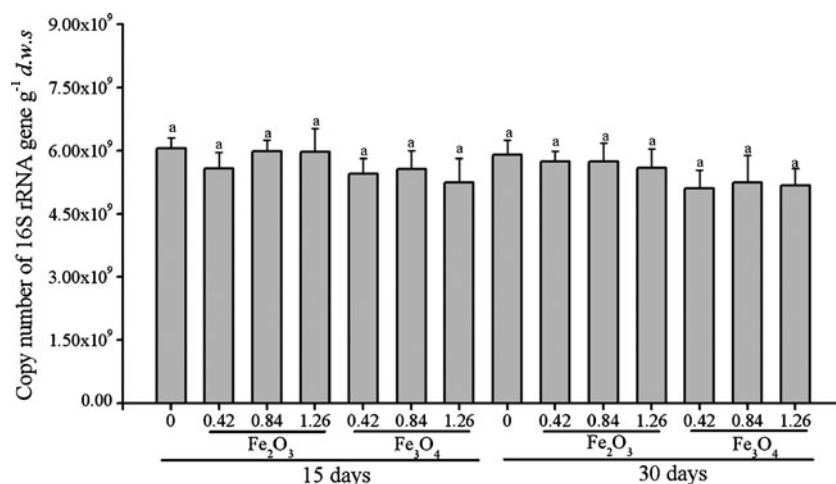
The release of nanoparticles to the soil is inevitable due to increased development of the nanomaterials industry, disposal of nano-containing consumer goods, utilization of nano-containing materials, etc. However, little knowledge is available to date about the effect of nanoparticles on soil environments. Identifying bacterial responses provides valuable information on the influence of nanoparticles on

soil health. In this study, agricultural soil is chosen because it is highly linked with human life. IOMNP-induced changes in bacterial community structure were observed using molecular approaches. Some DGGE band-related species could be stimulated by IOMNPs. PCA of PCR-DGGE fingerprinting profiles revealed varied effects of IOMNPs type and IOMNPs concentration on soil bacterial community composition. The total bacterial population size was basically stable, which was demonstrated by both qPCR and plate counting methods. Therefore, these genetic analyses provided molecular evidence that the concentrations of $\gamma\text{-Fe}_2\text{O}_3$ and Fe_3O_4 MNPs used herein seem to favour the growth of some bacteria in soil.

The impact of IOMNPs on the bacterial community could possibly be attributed to both the characteristics of nanoparticles (Ju-Nam and Lead 2008; Nowack 2009) and their contribution to the microorganism's metabolism. Due to their tiny size and stabilisation (He et al. 2006), IOMNPs can be easily transported into soil. Nano-metal oxides have enhanced surface-to-volume ratio (Waychunas et al. 2005); therefore, partial decomposition and release of ions is more likely for nanoparticles compared to the bulk material. Furthermore, nanoparticles have the most active surface sites (mainly Fe-OH site on IOMNPs (Liu et al. 2008)) that are able to bind to natural organic compound. For example, with the assistance of organic compounds in the soil, such as humic acids (HA) and fulvic acid (Illes and Tombacz 2006), IOMNPs addition could enhance the bioavailability of iron to the soil bacteria. HA is formed during the physicochemical and microbial degradation of plant and animal residues and is abundant in natural systems. It has a skeleton of alkyl and aromatic units that attach with carboxylic acid, phenolic hydroxyl and quinone functional groups, which could have strong affinity to the surface of IOMNPs. The absorption of HA on IOMNPs generally enhances their stability through a combination of steric and electrostatic effects. Additionally, due to ligand exchange reactions between HA and the surface sites of iron oxide, dissolved Fe (III) ions move into the aqueous phase from the surface of IOMNPs. Therefore, the bioavailable iron ions in soil are increased and would subsequently stimulate the growth of some microbes in soil.

Iron is an essential nutrient for almost all microorganisms because it plays an important role in optimum cell growth. Iron acts as a cofactor for a large number of enzymes, forms part of cytochromes and is required for many biochemical reaction, including respiration, photosynthetic transport, nitrate synthesis, nitrogen fixation and DNA synthesis. Microorganisms employ various iron uptake systems to secure sufficient supplies from their surroundings (Hantke 2001). Thus, IOMNPs treatment could provide beneficial nutrients for growth of some microbes in soil. As a consequence, the bacterial commu-

Fig. 5 The copy number of 16S rRNA gene from the soil sprayed with different concentrations of IOMNPs. Data are the mean of three determinations and the error bars indicate SD. Values are representative of three independent experiments. Three replicates were used in this experiment. Groups that are significantly different are indicated by different letters ($p < 0.05$)



nity composition would be changed and some DGGE band-related species could be stimulated. Several bacteria related to Actinobacteria, such as Duganella, Streptomycetaceae or Nocardioideae, could be stimulated under amendment with IOMNPs. Actinomycetes are one of the major groups of microbial populations present in soil (Kennedy and Gewin 1997). It has often been stated that they are active agents in the decomposition of organic matter, releasing carbon, nitrogen and ammonia, which supply plants with nutrients, and releasing cellobiose and various oligosaccharide intermediates as degradation products (Bahn et al. 1979). It also

has been reported that Actinomycete strains are able to improve plant growth and nutrition supply (Franco-Correa et al. 2010).

γ -Fe₂O₃ had a more beneficial impact on the soil bacteria community in this study. It has been suggested that iron-based nanoparticles are toxic due to the generation of reactive oxygen species (ROS). Previous studies have shown that chemically stable nanoparticles (γ -Fe₂O₃) have no apparent cytotoxicity, whereas nanoparticles containing either Fe²⁺ or Fe⁰ result in a dose-dependent decrease in the survival of *E. coli*, mainly due to oxidative stress. γ -Fe₂O₃

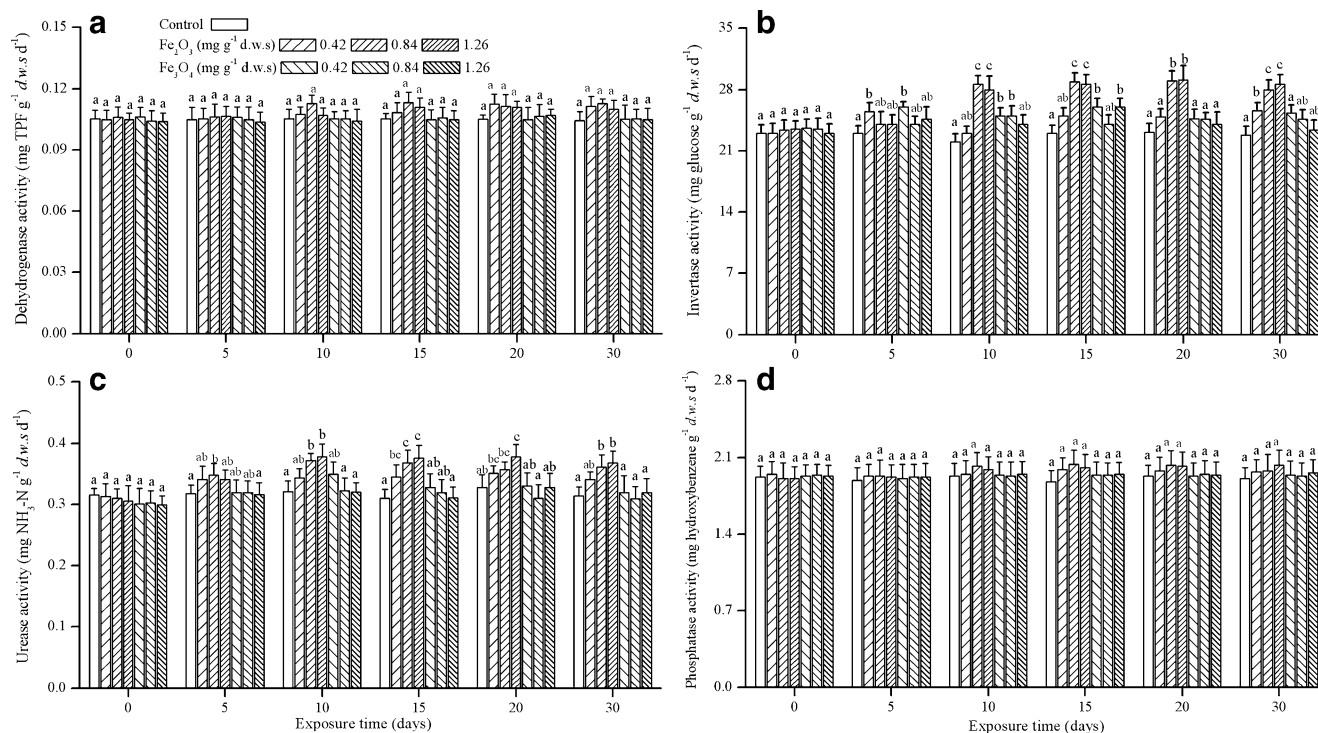


Fig. 6 Enzyme activities of dehydrogenase (a), invertase (b), urease (c) and phosphatase (d) of samples treated with different concentrations of IOMNPs (Fe₃O₄ and γ -Fe₂O₃) at different intervals. Bars

indicate the standard deviation of the mean. Groups that are significantly different are indicated by different letters ($p < 0.05$)

nanoparticles are composed of fully oxidised crystals and, consequently, are highly stable in the environment, indicating a lower capacity to generate oxidative stress. In contrast, Fe₃O₄ nanoparticles are unstable because of the high mobility of electrons within the structure and the diffusion of Fe²⁺. Reduced iron oxides are known to be efficient ROS producers (Auffan et al. 2008). Thus, the effect of IOMNPs could be counteracted by release of Fe²⁺ from Fe₃O₄, resulting in weaker enhancement of bacterial community richness and a smaller change in bacterial community composition.

Changes in the soil bacterial community could result in variation in soil enzyme activities. Soil enzymes play an essential role in matter and energy cycling in soil. Their activities represent the potential of the bacteria present in the soil to perform specific biochemical reactions. In this study, soil dehydrogenase, invertase, urease and phosphatase were investigated. Invertase and urease were both significantly stimulated by IOMNPs amendments, which could be caused by IOMNPs-induced changes in the bacterial community. As mentioned above, Actinomycetes-like species could be stimulated by IOMNPs. Because they facilitate the decomposition of organic matter, soil invertase and urease measured could be enhanced. Though soil enzymes are commonly investigated to characterize the states of soil ecosystem involved in elemental cycling, the stimulations in these enzymes reflect the speeding up of soil matters and energy cycling to some extent. Therefore, IOMNPs amendments could facilitate the turnover of C and N in soil. However, this positive effect of IOMNPs could only be on specific bacteria, not on whole soil microbes, because dehydrogenase, oxidative power of soil microorganisms, was not enhanced, which is consistent with the results of qPCR and plate counting. Furthermore, with its continuously elevated concentration due to increasing application of nanomaterials, the long-term influence of IOMNPs on the soil ecosystem is still not clear and probably an enigma. It is necessary to conduct further investigation of the long-term effects of IOMNPs and of other nanoparticles before we can draw a comprehensive conclusion about the effects of nanoparticles on the soil microbial ecosystem.

Acknowledgements This work was financially supported by National Natural Science Foundation of China (Project: 41001142, 60501009) and China-US International Science and Technology Cooperation Program (2009DFA31990).

References

- Auffan M, Achouak W, Rose J, Roncato MA, Chaneac C, Waite DT, Masion A, Woicik JC, Wiesner MR, Bottero JY (2008) Relation between the redox state of iron-based nanoparticles and their cytotoxicity toward *Escherichia coli*. *Environ Sci Technol* 42:6730–6735
- Bahn AN, Dirks OB, Destoppelaar JD, Huisintveld JHJ, Boom A, Hayashi JA (1979) Function of neuraminidases from oral Streptococci and Actinomycetes in the plaque-formation. *Caries Res* 13:86–87
- Colvin VL (2003) The potential environmental impact of engineered nanomaterials. *Nat Biotechnol* 21:1166–1171
- Dick WA, Cheng L, Wang P (2000) Soil acid and alkaline phosphatase activity as pH adjustment indicators. *Soil Biol Biochem* 32:1915–1919
- Feng YZ, Lin XG, Wang YM, Zhang J, Mao TT, Yin R, Zhu JG (2009) Free-air CO₂ enrichment (FACE) enhances the biodiversity of purple phototrophic bacteria in flooded paddy soil. *Plant Soil* 324:317–328
- Franco-Correa M, Quintana A, Duque C, Suarez C, Rodriguez MX, Barea JM (2010) Evaluation of actinomycete strains for key traits related with plant growth promotion and mycorrhiza helping activities. *Appl Soil Ecol* 45:209–217
- Ge Y, Schimmel JP, Holden PA (2011) Evidence for negative effects of TiO₂ and ZnO nanoparticles on soil bacterial communities. *Environ Sci Technol* 45:1659–1664
- Hantke K (2001) Iron and metal regulation in bacteria. *Curr Opin Microbiol* 4:172–177
- He F, Zhao D, Liu J, Roberts CB (2006) Stabilization of Fe-Pd nanoparticles with sodium carboxymethyl cellulose for enhanced transport and dechlorination of trichloroethylene in soil and groundwater. *Ind Eng Chem Res* 46:29–34
- Hu WB, Peng C, Luo WJ, Lv M, Li XM, Li D, Huang Q, Fan CH (2010) Graphene-based antibacterial paper. *Acs Nano* 4:4317–4323
- Illes E, Tombacz E (2006) The effect of humic acid adsorption on pH-dependent surface charging and aggregation of magnetite nanoparticles. *J Colloid Interf Sci* 295:115–123
- Janvier C, Villeneuve F, Alabouvette C, Edel-Hermann V, Mateille T, Steinberg C (2007) Soil health through soil disease suppression: Which strategy from descriptors to indicators? *Soil Biol Biochem* 39:1–23
- Jia ZJ, Conrad R (2009) Bacteria rather than Archaea dominate microbial ammonia oxidation in an agricultural soil. *Environ Microbiol* 11:1658–1671
- Ju-Nam Y, Lead JR (2008) Manufactured nanoparticles: An overview of their chemistry, interactions and potential environmental implications. *Sci Total Environ* 400:396–414
- Kanerva T, Palojarvi A, Ramo K, Manninen S (2008) Changes in soil microbial community structure under elevated tropospheric O₃ and CO₂. *Soil Biol Biochem* 40:2502–2510
- Kang S, Pinault M, Pfefferle LD, Elimelech M (2007) Single-walled carbon nanotubes exhibit strong antimicrobial activity. *Langmuir* 23:8670–8673
- Kasemets K, Ivask A, Dubourguier HC, Kahru A (2009) Toxicity of nanoparticles of ZnO, CuO and TiO₂ to yeast *Saccharomyces cerevisiae*. *Toxicol in Vitro* 23:1116–1122
- Kaye JP, McCulley RL, Burke IC (2005) Carbon fluxes, nitrogen cycling, and soil microbial communities in adjacent urban, native and agricultural ecosystems. *Glob Change Biol* 11:575–587
- Kennedy AC, Gewin VL (1997) Soil microbial diversity: Present and future considerations. *Soil Sci* 162:607–617
- Kirk JL, Beaudette LA, Hart M, Moutoglou P, Khironomos JN, Lee H, Trevors JT (2004) Methods of studying soil microbial diversity. *J Microbiol Meth* 58:169–188
- Klaine SJ, Alvarez PJJ, Batley GE, Fernandes TF, Handy RD, Lyon DY, Mahendra S, McLaughlin MJ, Lead JR (2008) Nanomaterials in the environment: Behavior, fate, bioavailability, and effects. *Environ Toxicol Chem* 27:1825–1851
- Kumar N, Shah V, Walker VK (2011) Perturbation of an arctic soil microbial community by metal nanoparticles. *J Hazard Mater* 190 (1–3):816–822

- Lee J, Mahendra S, Alvarez PJJ (2010) Nanomaterials in the construction industry: a review of their applications and environmental health and safety considerations. *Acs Nano* 4:3580–3590
- Liu JF, Zhao ZS, Jiang GB (2008) Coating Fe₃O₄ magnetic nanoparticles with humic acid for high efficient removal of heavy metals in water. *Environ Sci Technol* 42:6949–6954
- Liu SB, Wei L, Hao L, Fang N, Chang MW, Xu R, Yang YH, Chen Y (2009) Sharper and faster "nano darts" kill more bacteria: a study of antibacterial activity of individually dispersed pristine single-walled carbon nanotube. *Acs Nano* 3:3891–3902
- Meng H, Xia T, George S, Nel AE (2009) A predictive toxicological paradigm for the safety assessment of nanomaterials. *Acs Nano* 3:1620–1627
- Muyzer G, Dewaal EC, Uitterlinden AG (1993) Profiling of complex microbial populations by denaturing gradient gel electrophoresis analysis of polymerase chain reaction-amplified genes coding for 16S rRNA. *Appl Environ Microbiol* 59:695–700
- Nowack B (2009) The behavior and effects of nanoparticles in the environment. *Environ Pollut* 157:1063–1064
- O'Donnell AG, Seasman M, Macrae A, Waite I, Davies JT (2001) Plants and fertilisers as drivers of change in microbial community structure and function in soils. *Plant Soil* 232:135–145
- Perez JM, O'Loughin T, Simeone FJ, Weissleder R, Josephson L (2002) DNA-based magnetic nanoparticle assembly acts as a magnetic relaxation nanoswitch allowing screening of DNA-cleaving agents. *J Am Chem Soc* 124:2856–2857
- Sadowsky MJ, Schortemeyer M (1997) Soil microbial responses to increased concentrations of atmospheric CO₂. *Glob Change Biol* 3:217–224
- Schinner F, Vönmersi W (1990) Xylanase-activity, Cm-cellulase-activity and invertase activity in soil - an improved method. *Soil Biol Biochem* 22:511–515
- Sjogren CE, Johansson C, Naevestad A, Sontum PC, BrileySaebo K, Fahlvik AK (1997) Crystal size and properties of superparamagnetic iron oxide (SPIO) particles. *Magn Reson Imaging* 15:55–67
- Sondi I, Salopek-Sondi B (2004) Silver nanoparticles as antimicrobial agent: a case study on E-coli as a model for Gram-negative bacteria. *J Colloid Interf Sci* 275:177–182
- Tabatabai MA (1994) Soil enzymes. *Methods of Soil Analysis*. Soil Society of America, Madison
- Tamura K, Dudley J, Nei M, Kumar S (2007) MEGA4: Molecular evolutionary genetics analysis (MEGA) software version 4.0. *Mol Biol Evol* 24:1596–1599
- Tong ZH, Bischoff M, Nies L, Applegate B, Turco RF (2007) Impact of fullerene (C-60) on a soil microbial community. *Environ Sci Technol* 41:2985–2991
- Waychunas GA, Kim CS, Banfield JF (2005) Nanoparticulate iron oxide minerals in soils and sediments: unique properties and contaminant scavenging mechanisms. *J Nano Res* 7:409–433